Role of inviscid invariants in shell models of turbulence

L. Biferale[1] and R. M. Kerr[2]
[1]*Dipartimento di Fisica, Università "Tor Vergata" Via della Ricerca Scientifica 1, I-00133 Rome, Italy*
[2]*Geophysical Turbulence Program, National Center for Atmospheric Research, P.O. Box 3000, Boulder, Colorado 80307-3000*
(Received 31 July 1995)

Nonpositive definite, global inviscid invariants similar to helicity are discussed for two types of shell models, and evidence for an alternate role for helicity in Navier-Stokes turbulence is presented. It is suggested that the extra invariants play the role of triggering an intermittent cascade of energy to small scales characterized by pulses. These invariants also determine where a transition to chaos appears. An analysis of numerical experiments with existing models is suggested and a class of shell models where the dynamical interactions of a second quadratic invariant are closer to those of helicity in the Navier-Stokes equations is introduced. The place of the popular Gledzer-Ohkitani-Yamada model within this class is discussed.

PACS number(s): 47.27.Eq

I. INTRODUCTION

One of the outstanding questions in our understanding of fully developed turbulence is the mechanisms by which the cascade of energy to small scales is maintained. That the cascade is intermittent is well recognized, but the phenomenological and dynamical models used to address the problem are rarely connected to the dynamics in the full Navier-Stokes equations. In this paper it is shown that a popular model for explaining turbulent intermittency, the GOY model [1,2], shares some symmetries with terms in a decomposition of the spectral Navier-Stokes equations into the interactions between its helical components [3]. The essential common property that is defined in both the Gledzer-Ohkitani-Yamada (GOY) model and in the Navier-Stokes equations is the importance of interactions between components with oppositely signed helicity. This role for helicity supporting an intermittent cascade contrasts strongly with helicity's previously identified role in blocking the cascade [4,5], a role that was proposed earlier based on an analogy to the way magnetic helicity force-free states [6].

In the GOY model with the standard parameters for three-dimensional turbulence, interactions between modes with oppositely signed helicity occur naturally as the sign of helicity reverses between neighboring shells [7]. Whether Navier-Stokes turbulence follows a similar path is a more difficult question because there are several paths, characterized by interactions between different components of the helicity, that the cascade can follow. One way to investigate this question is to consider several variants of the GOY models that investigate each path in the full Navier-Stokes equations individually or in unison. One question would be how strongly the statistical behavior of the cascade depends on the symmetries in the different models. Another line of investigation is to determine which path the cascade follows in the full Navier-Stokes equations. In this paper, preliminary results following both of these approaches are presented, and the direction of a more complete study is presented. Also included will be an analysis of the Kerr-Siggia shell model [8], which has a cubic, nonpositive definite invariant that shares some dynamical properties with helicity, and served as an inspiration for part of this proposal. In all of these cases it will be argued that competition between the transfer of energy and the transfer of the generalized helicity could explain the presence of numerically observed chaotic dynamics and intermittency in the energy cascade. For the GOY models, results on intermittency corrections will be used to illustrate the importance of the second quadratic invariant in the energy cascade.

In Sec. II, results for the Kerr-Siggia model will be reported. In Sec. III, the GOY model is reviewed, and how the inviscid conserved quantities and the dynamics depend on the free parameters present in the model is discussed. In Sec. IV, an argument that predicts the transition from a trivial dynamics (dominated by the presence of an attractive fixed point) to a fully chaotic regime for some critical values of the free parameters is discussed. Some numerical results for the energy transfer are also discussed. In Sec. V, versions of the GOY model are introduced by considering explicitly the possibility of having shells which transport positive or negative helicity exactly as occurs in the Navier-Stokes equations. Two preliminary calculations with the full Navier-Stokes equations that support the importance of the interactions between components with oppositely signed helicity are presented. Some problems that can be studied by using the variants of the GOY model are discussed, and an analysis of the full Navier-Stokes equations that could be done to illuminate these properties is presented.

II. PULSE SCALING OF KERR-SIGGIA

The Kerr-Siggia model [8] is a shell model with one complex variable per shell, originating from a decimation of the possible interactions between triads in Burgers equation. With a simple forcing and eddy viscosity the equations were

$$du_1/dt=\epsilon/u_1^*+2iu_2u_1^*\ ,$$
$$du_n/dt=k_{n-1}i(u_{n-1}^2+2u_{n+1}u_n^*)\ , \quad (1)$$
$$du_N/dt=k_{N-1}i(u_{N-1}^2+\nu_e|u_N|u_N)\ ,$$

where ϵ was the average energy input and dissipation, ν_e was taken to be $2^{2/3}$, and $k_n=2^n$. Defining

$$E_n=\tfrac{1}{2}u_nu_n^*$$
$$H_n=\mathrm{Re}(u_n^*u_{n-1}^2) \quad (2)$$
$$A_n=\mathrm{Im}(u_n^*u_{n-1}^2)$$

for $\epsilon=\nu_e=0$, there are two inviscid invariants $E=\sum E_n$ and $H=\sum H_n$. The first is energy and the second, while not positive definite, can be treated as a Hamiltonian with canonical variables u_n and $u_{-n}=u_n^*$ as follows:

$$du_n/dt=ik_n\delta H/\delta u_{-n}\ . \quad (3)$$

The energy transfer between shells is $\epsilon_n=-k_{n-1}A_n$. There is a trivial, unstable Kolmogorov solution with $u_n=-i(2^{1/3}\epsilon)^{1/3}k_n^{-1/3}$, $H_n=0$, and $E_n=2^{2/9}\epsilon^{2/3}k_n^{-2/3}$ corresponding to a solution of an earlier cascade model [9].

The context for discussing this model along with the GOY model and the Navier-Stokes equations is the extra invariant H. Despite the fact that this H is cubic and not quadratic, and that neither Euler nor GOY has a Hamiltonian of this form, due to the nonpositive definite nature of H, it appears to have some of the same qualitative effects upon the cascade that we speculate helicity is capable of for Navier-Stokes and GOY models. The point is that while additional invariants can block the energy cascade, as enstrophy does in two dimensions and helicity does to some degree in Navier-Stokes [4,5], due to the nonpositive definite nature of the invariant there is an escape route where the cascade can find a way around this blockage. As will be demonstrated for the Kerr-Siggia model, this can take the form of pulses. From the tools used to demonstrate this for the Kerr-Siggia model, it will then be demonstrated that there is weak evidence for analogous phenomena in Navier-Stokes.

In the original discussion [8], two classes of solutions besides the trivial Kolmogorov solution were discussed. First, stationary solutions for a small number of shells with no forcing or dissipation ($\epsilon=\nu_e=0$) and maximal H were discussed. Second, forced, dissipative solutions were discussed. Intermittency was found in the time-dependent solutions, and the effect of the extra invariant was noted, particularly as it affected the slope of the energy spectrum, which was $\langle E_n\rangle\sim k_n^{-1/2}$ rather than the Kolmogorov solution, but what effect the stationary solutions might exert upon the forced, dissipative time-dependent solutions was not considered.

For the present calculations, $\epsilon=1$ was chosen, which gives a characteristic time scale of $t=1$. Using as initial conditions $u_1=u_2=(1,1)$, $u_n=0$, $n\geq 3$, and $N=14$, it took until $t=3.9$ for the effects of initial transients to disappear. Then statistics were taken until $t=6.8$. Figure 1 shows the spectra of $\langle E_n\rangle$ and $\langle H_n\rangle$ for this period as well as $k_n^{-1/2}$ curves, confirming the results of the original paper [8]. Details will be discussed after the evidence for pulses is presented.

Figure 2 shows E_n and H_n spectra for a series of moderately spaced times, and the time development of E, H, and dissipation for this time period. By "moderately spaced in time" it is meant that the times shown are not so closely spaced so as to show continuous development, but are close enough to show a relationship between pulses of E_n and H_n and intermittent bursts in the dissipation.

The primary event to focus upon is best illustrated in the H_n spectra. In this sequence it starts as a pulse of positive H_n centered on $n=4$ at $t=6.11$. This is associated with only one of several bumps in the energy spectrum at this time, and is not associated with the spike in energy dissipation at $t=6.15$. This spike in energy dissipation is associated with one of the higher shell bumps in the energy spectrum, and comes from a pulse at an earlier time of oppositely signed H_n similar to the pulse to be described.

Following the appearance of the positive peak of H_n in $n=4$ at $t=6.11$, this peak breaks off from the lower shells and slowly propagates to larger shell numbers. The energy peak associated with it moves in tandem. Spectra of the transfer rates of E_n and H_n also have peaks that move with the pulse. When the effects of the highest shell, where the dissipation occurs, are felt, the pulse stalls at $t=6.29$ before the energy in the pulse suddenly dissipates at $t=6.34$. The stalling is the probable source of the bump in the time-averaged energy spectra just before the dissipation regime. While this bump is on top of a spectrum less steep than Kolmogorov ($k_n^{-1/2}$ rather than $k_n^{-2/3}$), it is qualitatively similar to a bump in the turbulent energy spectra for atmospheric observations [10], spectral closures [4], and forced calculations of

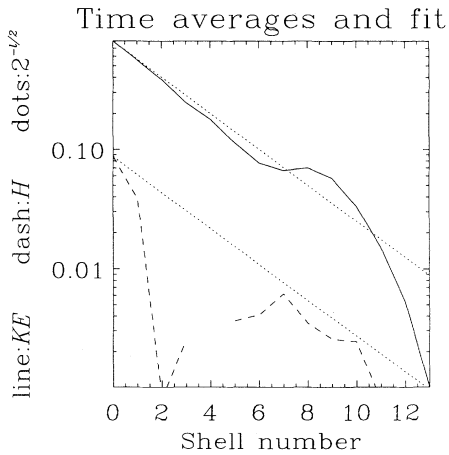

FIG. 1. Time-averaged spectra for the kinetic energy (solid line) and Hamiltonian (dashes) for the Kerr-Siggia model. Note the "bump" in the energy spectra near shell 9. The gap in the Hamiltonian spectra at shell 4 is where it is negative. $2^{-n/2}$ curves are drawn for comparison.

Navier-Stokes turbulence [11]. For Navier-Stokes the bump is believed to be associated with a bottleneck effect [32], where the decrease in the slope of kinetic energy spectrum in the dissipation regime blocks the free flow of kinetic energy just at the boundary between the inertial and dissipation subranges. While this effect probably plays some role in the appearance of the bump in the Kerr-Siggia model, examination of Fig. 2 suggests a strong role for the stationary solutions associated with the second invariant. This comes from noticing that the cubic invariant is nearly maximal over the shells covered by the bump.

While this pulse is dissipating at $t=6.34$, the next major pulse of negative H_n is beginning to move into shell 2 and positive H_n for the major pulse following that is developing in shell 0 from the forcing. So a succession of E_n and alternately signed H_n pulses is suggested. Clearly this is a simplified picture, as there are minor spikes in dissipation between the major spikes that are associated with weak pulses with small H_n of no particular sign. An example of such a weak pulse is the blip in H_n at $n=8$ for $t=6.35$ and the rapidly moving E_n at this time. To quantitatively demonstrate the alternation in sign of the strong pulses, Fig. 3 is a contour plot in shell and time separation of correlations between different shells and times of E_n and H_n. These plots are similar to contour plots of the energy transfer in forced Navier-Stokes calculations [12,13], and in meteorology are referred to as Hovmüller diagrams. These are

$$\langle (F_{n+\Delta_n,t+\Delta t}-\overline{F_{n+\Delta_n}})(F_{n,t}-\overline{F_n})\rangle \ , \tag{4}$$

where F_n is either E_n or H_n. Positive correlations are dark, negative are light. These plots are for $n=1$, the second shell. The effect of a single pulse is the first region of increasing Δ_n and Δt originating at (0,0). The propagation is linear after the first few shells. Starting at about $\Delta t=0.5$ there is another strong dark region in the E_n correlation, and a strong light region in the H_n correlation. This supports the qualitative picture coming from watching the time development in Fig. 2 that there are a succession of pulses of oppositely signed H_n.

The appearance of these pulses raises several questions. First, what modification of the stationary solutions can

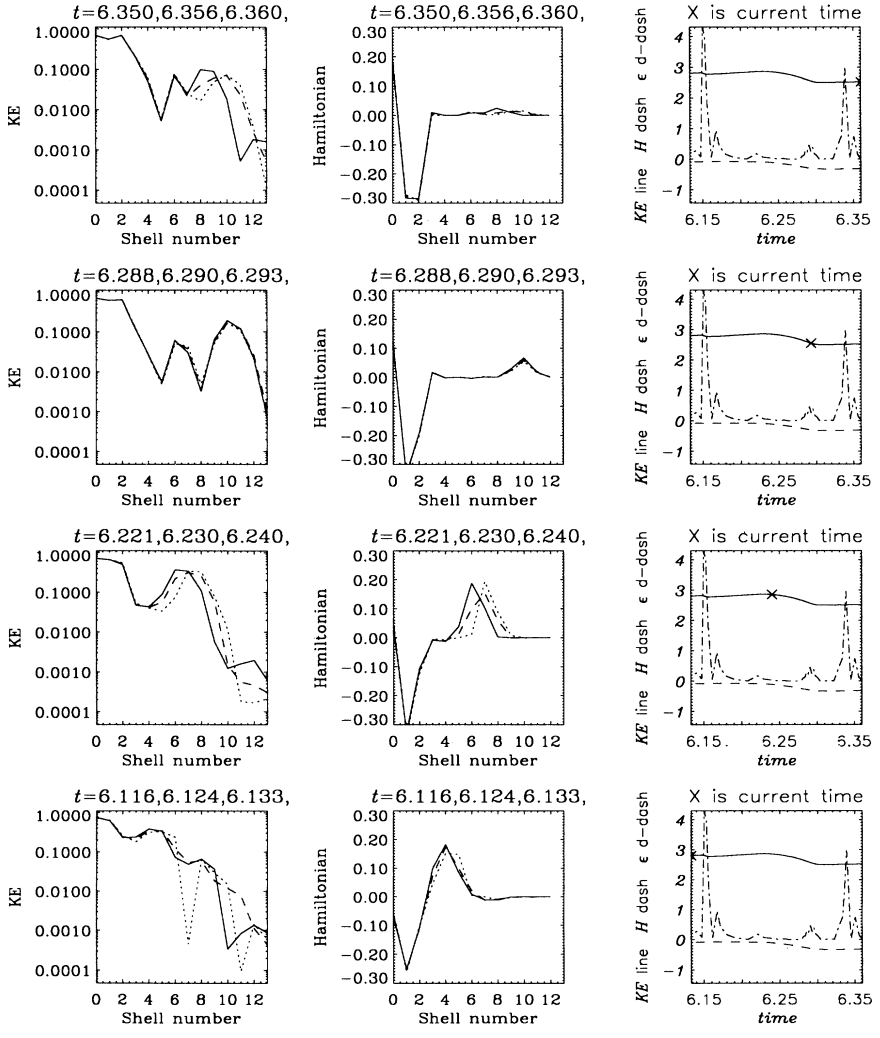

FIG. 2. Spectra at individual times for the kinetic energy and Hamiltonian. In order, the times correspond to the first time: ——; second time: — — —; and third time: · · · . Also given is the time evolution of the total kinetic energy ——; Hamiltonian — — —; and energy dissipation · · · for the period covered by the spectra. The **X** in the energy curves indicates roughly the times of the spectra to the left.

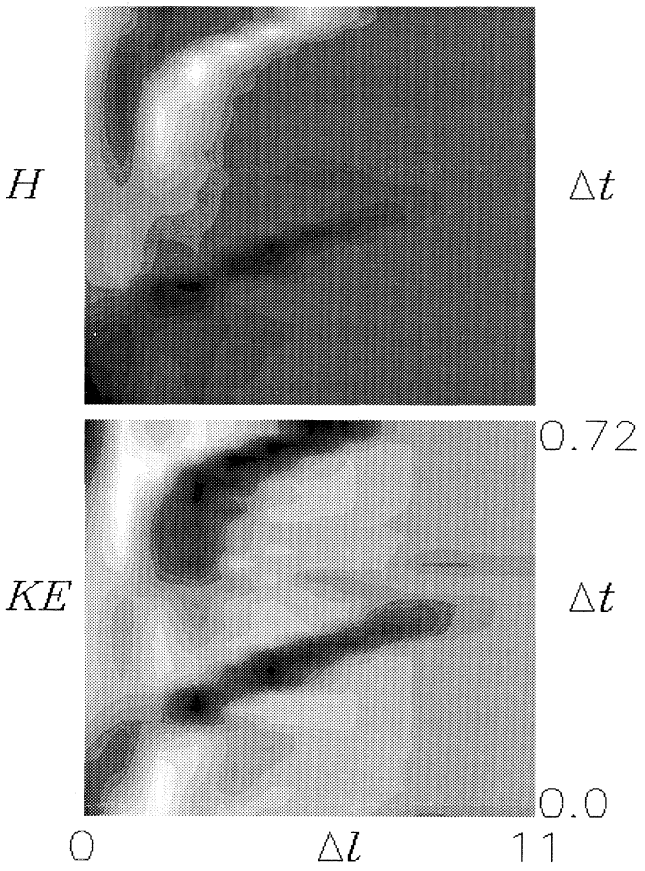

FIG. 3. Hovmüller diagrams in shell and time separation of kinetic energy and Hamiltonian fluctuations at different shell numbers and times using (4). Negative fluctuations correlation are light, positive are dark. Note the strong black for energy is not at (0,0), indicating that the strongest fluctuations in energy are in the higher shells. The sign of H fluctuations changes between pulses (light upper ridge), but does not for energy (dark upper ridge).

propagate as a unit? Second, what causes the alternation in sign of H_n of the pulses; is it the forcing or the nonlinear dynamics? We will not attempt to answer these questions. The point we do want to make is that there is some connection between the alternation in sign of the extra nonpositive definite conserved quantity that seems to be associated with the appearance of pulses in the energy cascade and with intermittency in the model. In calculations where the extra invariant is suppressed, intermittency disappears. These ideas are supported by noting that the mechanism by which the conserved quantities are pumped in the system and removed from the system can influence the scaling laws in the inertial subrange [15,16]. An extreme example is a calculation of the Kerr-Siggia model with a Newtonian viscosity [15] where the extra conserved quantity is suppressed, where there is a Kolmogorov spectrum and no intermittency. These are subtle questions that would require more accurate studies.

How can the pulses be related to the spectra in Fig. 1? The $\langle E_n \rangle$ spectrum in Fig. 1 goes as $2^{-n/2}$. By dimensional arguments one might expect that the $\langle H_n \rangle$ spectrum would obey $2^{-3n/4}$, but this is not required since at any given time $\langle H_n \rangle$ can have either sign. In fact, the $\langle H_n \rangle$ spectrum is less steep than this and also seems to follow $2^{-n/2}$. To understand this, imagine that each pulse is a coherent package of E_n and H_n traversing the spectrum, spending on average $2^{-n/2}$ time in each shell. Then the time-averaged spectra $\langle E_n \rangle$ and $\langle H_n \rangle$ will both have $2^{-n/2}$ spectra. This is similar to the argument that has been used to generate a $-\frac{5}{3}$ spectrum from fluctuations in a strained Burgers vortex [17]. If Δt spent in each band goes as $2^{-n/2}$ as this suggests, then this would imply that the bands in the $(\Delta_n, \Delta t)$ plots should approach zero slope as Δ_n increases. There is some tendency in this direction for small Δ_n in Fig. 3, but for larger Δ_n when the stalling noted at $t=6.29$ in Fig. 2 and dissipation effects are important, the bands are nearly linear. Again, the time-averaged $\langle H_n \rangle$ should not have any particular sign, as evidenced by shell 4 in Fig. 1, and their magnitude $|\langle H_n \rangle|$ should decrease as the averaging time is lengthened. This has been verified by using different time intervals for the time averaging.

III. GOY MODEL

Given this discussion, let us now examine properties of the Kerr-Siggia model shared by the GOY model [1,2]. The GOY model has a very rich dynamical behavior, and has been the object of many studies in recent years (see

[7,18–22] for some numerical and analytical results). It is the most popular shell model for three-dimensional (3D) turbulence, because its intermittent properties are very close to the corresponding quantities in Navier-Stokes equations when the parameters of the nonlinear terms share some properties with the nonlinear term in the Navier-Stokes equations. In particular, for zero viscosity and no external forcing, when the system has the same conservation laws as a 3D flow: conservation of energy, helicity, and volume in phase space.

The dynamical equations are as follows:

$$\frac{d}{dt}u_n = ik_n(u^*_{n+1}u^*_{n+2} + bu^*_{n+1}u^*_{n-1} + cu^*_{n-1}u^*_{n-2}) - \nu k_n^2 u_n + \delta_{n,n_0} f \tag{5}$$

where ν is the viscosity and f is a forcing acting on a large-scale shell (for example, $n_0=1$) introduced to obtain a statistically stationary dynamical state. This model has interactions only between first- and second-neighbor shells in the Fourier space. The two parameters b and c in the nonlinear terms are chosen such as to conserve energy, $E=\sum_n |u_n|^2$ for any choice of λ. The most general choice of parameters is

$$b=-\frac{\epsilon}{\lambda}, \quad c=-\frac{1-\epsilon}{\lambda^2}, \tag{6}$$

where ϵ is the second free parameter in the model.

The GOY model also has a second quadratic invariant besides energy:

$$H=\sum_n \chi(\epsilon)^n k_n^{\alpha(\epsilon,\lambda)}|u_n|^2 . \tag{7}$$

While energy conservation is forced by choice (6), the characteristics of the second invariant H change by changing the values of ϵ and λ. When $\epsilon<1$ this second invariant is not positive definite [$\chi(\epsilon)=-1$], while if $\epsilon>1$ it is positive definite [$\chi(\epsilon)=+1$]. By remembering that the Navier-Stokes equations are characterized by having a second inviscid invariant that is positive definite in 2D (entrophy), and nonpositive definition in 3D (helicity), the value $\epsilon=1$ can be identified as the border between a shell model for 2D turbulence ($\epsilon>1$) and a shell model for 3D turbulence ($\epsilon<1$). In the following, the problem of whether shell models like GOY model are a good representation of 2D turbulence [23] is not addressed, and only the range ($0<\epsilon<1$) where the dynamics should reproduce aspects of a 3D turbulent flow will be considered.

By looking in detail at the structure of the second invariant, only when $\alpha(\epsilon,\lambda)=1$ does it have physical dimensions coinciding with Navier-Stokes helicity [7]. This defines a line in the plane of free parameters where the inviscid conservation laws of the GOY model are very similar to the 3D Navier-Stokes equations. Because this invariant has the same physical dimensions as 3D helicity and is nonpositive, we will denote it as the GOY helicity in the following. In Sec. VI, a modified version of the GOY model will be introduced with a second invariant having more correspondence with fluid helicity.

A necessary point before going on is that model (5) has two inviscid fixed points corresponding to the Kolmogorov scaling $|u_n|\sim k_n^{-1/3}$ (constant flux of energy, zero flux of helicity) and to a fluxless scaling $|u_n|\sim k_n^{-(1+\alpha)/3}$ (constant flux of helicity, zero flux of energy) [21].

For this study our interest in this model comes from the presence in the (ϵ,λ) plane of a region where the static Kolmogorov-like fixed point is dynamically unstable [21]. The dynamics is fully chaotic, and shows an intermittent cascade of energy toward small scales [18,20] with a complex (multifractal) structure of the attractor in the phase space. This intermittency is quantified by measuring the scaling exponents $\zeta(p)$ for the structure functions in the inertial range

$$S_p(k_n)=\langle |u_n|^p \rangle \sim k_n^{\zeta(p)} . \tag{8}$$

Only very recently [7,22] has it been realized that the second quadratic invariant plays a crucial role in the dynamics of the model. In [7], it was found by varying the two free parameters (ϵ,λ) in the 3D physically relevant region ($0<\epsilon<1;\lambda>1$) that, along the line of constant helicity [$\alpha(\epsilon,\lambda)=1$], the model has the same intermittent behavior. That is, the set of $\zeta(p)$ depends only on the value of α, giving numerical evidence that the dynamics of the model is strongly dependent on the presence of the second inviscid invariant. Furthermore, it has been shown [22] that by modifying the nonlinear term such as to destroy the presence of the second invariant (but still preserving the inviscid energy conservation) the intermittent corrections to $K41$ seem to weaken.

IV. TRANSITION TO CHAOS

It has been shown [21] that by fixing λ and varying the ϵ parameters (and, therefore, by changing α) the GOY model undergoes a transition to chaos following a Ruelle-Takens scenario. In particular, there exists a critical value ϵ_c such that for $\epsilon<\epsilon_c$ the Kolmogorov fixed point $u_n\sim k_n^{-1/3}$ is dynamically stable. Extending this analysis by changing the ratio between shells in the range $1<\lambda<3$, it is found that the Ruelle-Takens transition is quite general [24]: there exists a line in the plane (ϵ,λ) which divides the region where a Kolmogorov-like fixed point is dynamically stable from a region where the dynamics is chaotic and intermittent. This qualitative trend of the transition line appears to be universal, even if the exact location can be slightly influenced by the forcing and by the value of viscosity. In the following, a very simple argument is presented based on the presence of the second nonpositive invariant that predicts, with good accuracy, the existence of the transition and its location for any value in the plane (ϵ,λ).

Consider the two inviscid quadratic invariants, the energy and the generalized helicity, and their currents. First, for zero viscosity and zero forcing energy, conservation gives

$$\frac{d}{dt}|u_n|^2 = J_{n-1}-J_n , \tag{9}$$

where the energy current

$$J_n=\mathrm{Im}[-\Delta_{n+1}-(1-\epsilon)\Delta_n] \tag{10}$$

is defined in terms of triple correlations:

$$\Delta_n = k_{n-1} u_{n-1} u_n u_{n+1} \ . \tag{11}$$

The second conservation law for helicity takes the form

$$\frac{d}{dt}(-)^n k_n |u_n|^2 = L_{n-1} - L_n \ , \tag{12}$$

where the current of helicity L_n from the nth shell to the $n+1$th shell is

$$L_n = (-)^n k_n \mathrm{Im}[\Delta_n - \Delta_{n+1}] \ . \tag{13}$$

Let us suppose, for the moment, that there exists only one conserved quantity: energy. Then, very standard arguments [25] tell us that if viscosity is zero, the system tends to equipartition, corresponding in the GOY model to $|u_n|^2 = \text{const}$. If one switches on viscous effects, and starts with an initial configuration with energy concentrated in the first shells, an energy cascade toward small scales develops. This energy cascade has been interpreted as the attempt of the system to reach another equipartition state [25]. This attempt at restoring equipartition is frustrated by viscous dissipation at small scales that continuously removes energy, and prevents the small scales from reaching an equilibrium or quasiequilibrium state.

The Kolmogorov 1941 cascade, describing a smooth and constant transfer of energy from large scales to small scales, is another way to rephrase this mechanism. But why does the flow not follow this picture of relaxing to a smooth and homogeneous transfer of energy, instead preferring to use a highly intermittent cascade consisting of bursts and blockages which are the origins of the intermittent corrections to the $\zeta(p)$ exponents? This is where we are proposing that the second inviscid quadratic quantity enters into the picture.

It is well known that in 2D turbulence the presence of a second positive definite quadratic invariant (entrophy) does not allow the energy to cascade forward (toward small scales) [26]. This is a general result; *either* the two conserved quantities must transfer in different directions in Fourier space, *or* only one can transfer to small scales. For example, in 2D turbulence it is widely believed that there exists a forward transfer of entrophy and a backward transfer of energy (inverse cascade).

In contrast, the presence of a second nonpositive definite quadratic invariant, like helicity in 3D turbulence, is only a minor constraint on the forward transfer of energy. Moreover, it is a constraint that, due to the nonpositiveness, can have strong spatial and temporal fluctuations. If this picture is correct, intermittency in the 3D energy transfer could be the result of a competition between energy and helicity cascades. Temporal and/or spatial intermittency in the energy flux would be the result of switching between a net transfer of energy (possible due to cancellation effects in the helicity flux) and a depletion in the energy transfer due to the presence of a nonzero helicity flux.

How can these phenomenological ideas be checked in the GOY model? In the GOY model, a smooth and nonintermittent energy transfer would correspond to dynamics near the Kolmogorov manifold $u_n \sim k_n^{-1/3}$. This implies that the energy flux (9) is almost constant in the inertial range, and that the helicity flux (12) is almost vanishing. This Kolmogorov behavior is obtained when the model has a static stable fixed point. It is natural, then, to ask if it is possible to understand the transition from the static behavior to chaotic dynamics by invoking the second invariant. By plugging the Kolmogorov solutions into the expression for the generalized helicity (7), we obtain

$$H = \sum_n \chi(\epsilon)^n k_n^{\alpha(\epsilon,\lambda)-2/3} \ . \tag{14}$$

It is therefore clear that, whether the exponent $(\alpha - \frac{2}{3})$ in (14) is positive or negative determines whether H receives most of its important contribution from small or large scales, respectively. Therefore, when $\alpha > \frac{2}{3}$ the second invariant is concentrated at small scales and, as in 2D turbulence, prevents a smooth forward transfer of energy. This is reflected by strong intermittency and large deviations from Kolmogorov scaling. However, one can imagine that from time to time it is still possible to transfer energy if some cancellation effects lead to an almost zero H flux. On the other hand, when $\alpha < \frac{2}{3}$, energy transfers toward small scales without having any relevant change in H, i.e., the model relaxes in to a trivial Kolmogorov-like fixed point.

Figure 4 shows the numerical results [24] for the transition from a static Kolmogorov behavior to chaotic dynamics by changing ϵ and λ. As predicted, the transition happens near the critical line defined by

$$\alpha(\epsilon_c, \lambda_c) = \tfrac{2}{3}, \quad \lambda_c = (1 - \epsilon_c)^{-3/2} \ . \tag{15}$$

The systematic shift of 5% between prediction (15) and the numerical results is probably due to viscosity as previously discussed [24]. We believe that this very simple result is confirmation that the dynamics of the model is strongly influenced by the second invariant.

Figure 5 shows decaying numerical experiments; that is, zero forcing and nonzero viscosity with energy initial-

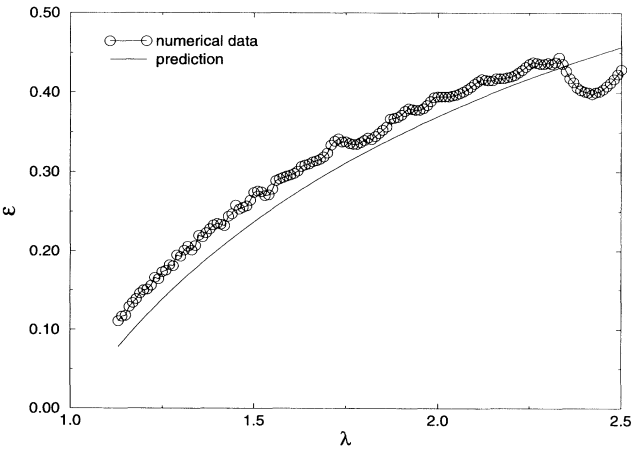

FIG. 4. Comparison in the (ϵ, λ) plane of the numerically estimated, transition (circles) [21] and the theoretical prediction (solid line).

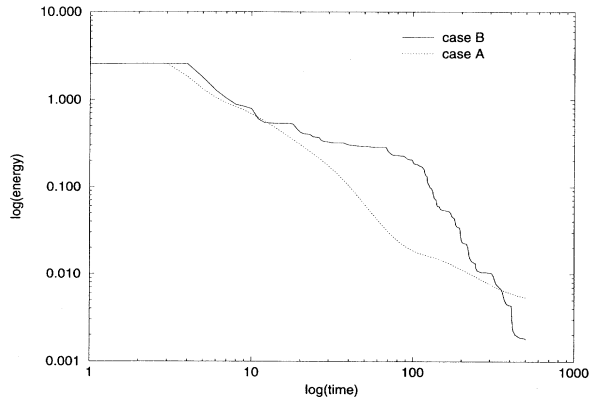

FIG. 5. Log-log plot of the total energy as a function of time in a pure decaying simulation. Case A (dotted line) corresponds to a smooth Kolmogorov-like transfer of energy, while case B (solid line) corresponds to a chaotic intermittent energy transfer.

ly concentrated at large scales, that compare the dynamical behavior of the model in two characteristic regions: case A ($\epsilon=0.1,\lambda=2$), where there is smooth energy-transfer regime (on the right side of the critical curve in Fig. 4) and case B ($\epsilon=0.5,\lambda=2$), where the dynamics is chaotic and intermittent (left side of the curve in Fig. 4). What is interesting is that, for case A, when the second invariant does not introduce any constraint in the energy transfer ($\alpha<\frac{2}{3}$), the energy dissipation is a smooth function. This means that energy is transferred through the inertial subrange without any blocking and with a power-law behavior in time. However, in case B ($\alpha>\frac{2}{3}$), the energy dissipation has a staircase shape in time, indicating long periods when little energy reaches small scales (blocking) interrupted by short bursts of dissipation. This would be consistent with the suggested role for helicity, where in addition to blocking the transfer, cancellation in the helicity transfer is associated with strong dissipation events.

Figure 6 shows the time evolution of the energy current J_n and the helicity current L_n through a shell in the inertial range where the model is chaotic. Obviously, the two fluxes are correlated, but the interesting fact is that when there is a burst of energy, the helicity flux has a sinusoidal shape, i.e., a net forward transfer of energy is only possible if the net averaged transfer of helicity is zero. Expanding upon the earlier proposal, this suggests blocking of energy transfer due to competition with helicity, interrupted by strong dissipation events made possible by brief, intermittent periods of large helicity fluctuations, but no net helicity flux. The dissipation events might then be associated with a strong dynamical coupling between modes with oppositely signed helicity, which would permit large helicity fluctuations, but no net helicity flux.

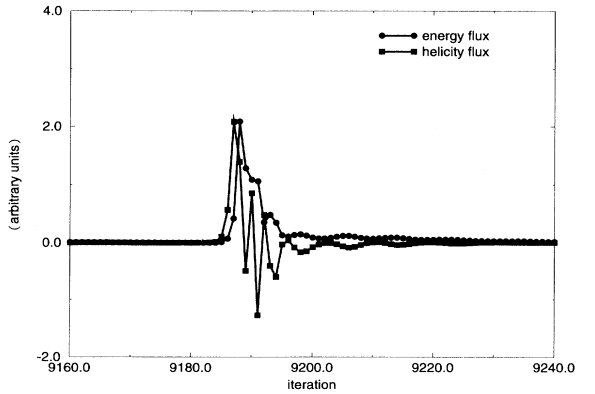

FIG. 6. Fluxes of energy and helicity during a burst through a shell in the inertial range. Notice the oscillatory behavior of the helicity flux triggering the energy transfer.

V. SHELL MODEL

As described in Sec. IV, the structure of what we call helicity in the GOY model is only partially consistent with the helicity in the Navier-Stokes equations. Apart from the observation that it has the right dimensions and that it is not positive definite, there is an asymmetry between odd and even shells that does not any counterpart in physical flows. One means of overcoming this problem is to introduce two dynamical variables in each shell, one transporting positive helicity u_n^+ and the other transporting negative helicity u_n^-. The next step is choosing how to couple these terms. For this, we will use a complete decomposition of the three-dimensional Navier-Stokes equations [3] into a basis where the two independent components of the velocity field at each wave number correspond to two pure helical waves. In such a basis there are four possible independent classes of triads interactions distinguished by the combination of helicity transported from each one of the three interacting modes.

Let us fix, for simplicity, the three modes $\mathbf{q}$, $\mathbf{p}$, and $\mathbf{k}$ such that $|\mathbf{k}|<|\mathbf{p}|<|\mathbf{q}|$, and call $u_{s_k}(\mathbf{k})$, $u_{s_p}(\mathbf{p})$, and $u_{s_q}(\mathbf{q})$ the three interacting modes, where $(s_k,s_p,s_q)=(\pm1,\pm1,\pm1)$ refer to the sign of helicity in each mode. Then it is simple to show that each triad can fall into one of the four following classes:

(1) $(s_k,s_p,s_q)=(+,+,+)$ or $(-,-,-)$.

(2) $(s_k,s_p,s_q)=(+,+,-)$ or $(-,-,+)$.

(3) $(s_k,s_p,s_q)=(+,-,-)$ or $(-,+,+)$.

(4) $(s_k,s_p,s_q)=(-,+,-)$ or $(+,-,+)$.

Following this decomposition, one is led naturally to introduce four classes of shell models, each one corresponding to one of the four independent classes of triad interaction present in the Navier-Stokes equations.

What is quite remarkable is that the original GOY model belongs to one of these classes (the fourth). To demonstrate this, we write the general equation for this class using positive helicity shells u_n^+ and negative helicity shells u_n^-,

$$\frac{d}{dt}u_n^+ = ik_n(u_{n+1}^- u_{n+2}^+ + bu_{n+1}^- u_{n-1}^- + cu_{n-1}^- u_{n-2}^+)^* - \nu k_n^2 u_n^+ + \delta_{n,n_0} f^+ ,$$
$$\frac{d}{dt}u_n^- = ik_n(u_{n+1}^+ u_{n+2}^- + bu_{n+1}^+ u_{n-1}^+ + cu_{n-1}^+ u_{n-2}^-)^* - \nu k_n^2 u_n^- + \delta_{n,n_0} f^- , \quad (16)$$

for which the conserved energy and helicity are given by

$$E = \sum_n |u_n^+|^2 + |u_n^-|^2 , \quad (17)$$

$$H = \sum_n k_n(|u_n^+|^2 - |u_n^-|^2) \quad (18)$$

exactly as in the Fourier-helicity decomposition of Navier-Stokes equation [3]. By noticing that in the original GOY model shells n and $n+2$ have the same GOY helicity, it can be seen that (16) is formed from two masked and uncorrelated versions of the original GOY model for the dynamical evolution of the variables $(u_1^+, u_2^-, u_3^+, \ldots, u_{2n-1}^+ u_{2n}^-)$ and $(u_1^-, u_2^+, u_3^-, \ldots, u_{2n-1}^-, u_{2n}^+)$. Therefore (16) has, by definition, the same behavior as the previous model. From this, we think it is of primary importance to study in details the dynamical behavior of the other three shell models (corresponding to classes 1, 2, and 3), allowing helicity to have all the dynamical interactions found in Navier-Stokes. Work in this direction is in progress, and will be reported elsewhere [28].

VI. NAVIER-STOKES HELICITY

Up to this point only ideal shell models with extra non-positive definite invariants have been considered, as well as how they might be extended to more closely resemble to helicity interactions in the Navier-Stokes equations. We would like to relate these ideas directly to the Navier-Stokes equations. As noted, earlier attempts at understanding the effects of helicity have emphasized its power to block the cascade [4,5]. However, despite the blocking power of the extra invariant, the shell model calculations are indicating that the cascade can proceed through interactions between shells where the sign of the extra invariant is opposite. In a full calculation, we would also want to see what the effects of helicity in physical space are. For example, there are low Reynolds number Navier-Stokes calculations of how vortex rings link and unlink and can generate and destroy helicity [29,30]. Because spectral properties were not analyzed and because of the low Reynolds numbers of these simulations, strong conclusions about the effects of helicity cannot be made from these calculations. But it can be said that even though the initial conditions contained large-scale helicity, small-scale structures appeared, and production of helicity from viscous effects was not strongly blocked.

Therefore, initial conditions that contain significant large-scale helicity, but which show more clearly how a cascade is not blocked, would be desirable. Whether or not production of small-scale helicity by anisotropies plays a role, as has been suggested [31], will not be our objective. Simulations of isotropic, homogeneous tur-

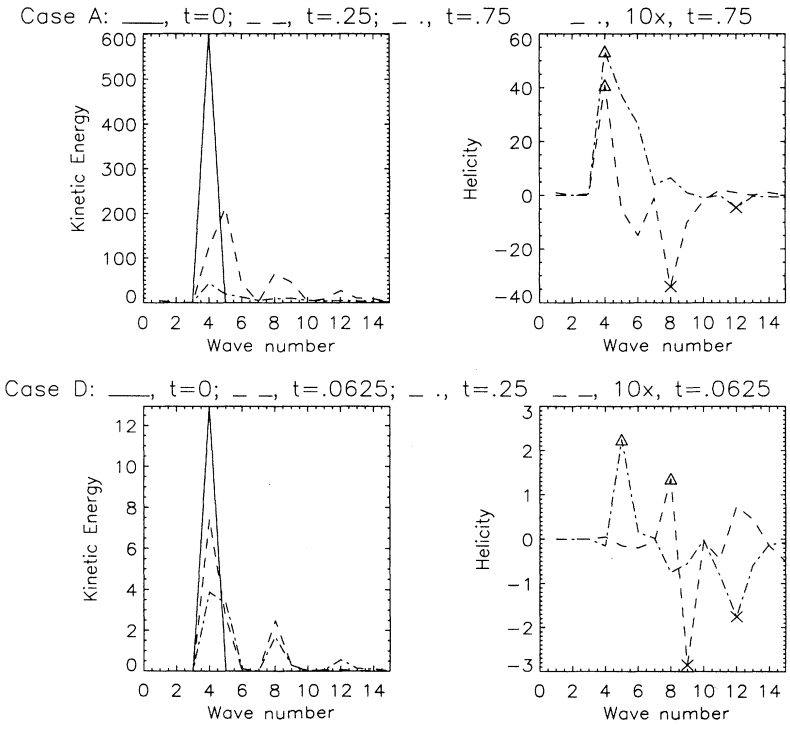

FIG. 7. Navier-Stokes three-dimensional banded wave spectra of the kinetic energy and helicity at individual times. At $t=0$ only energy is shown for each case. For case A, the helicity at the later time ($t=0.75$) is multiplied by 10. For case D, the helicity at the earlier time ($t=0.0625$) is multiplied by 10. Triangles indicate helicity maxima at the two times for each case, and crosses indicate helicity minima.

bulence in a periodic box are traditionally initialized with a given spectrum, but the phases of individual wave numbers is completely random. To test the effects of helicity, we propose constraining the phases of the velocity components such that the helicity of the Fourier modes is not all of one sign, unlike the investigations of the blocking power of helicity [5]. Since shell models indicate strong effects from extra invariant fluctuations even when the average value is zero, this suggests initializing a Navier-Stokes calculation with net zero helicity.

Several tests of this type have been done, all with one qualitatively similar feature. Helicity when it first appears in the spectra pops up in two neighboring bands of opposite signs; then the bands separate. Other than this qualitative feature, the number of tests is not yet sufficiently large to make definitive statements. Two cases are shown in Fig. 7. Both cases are 64^3 simulations, where only a small number of modes in wave number band 4 were initialized. Each has the common feature noted, but a rich variety of additional features as well.

In case A, each mode is initialized with maximal helicity, but otherwise the phases were chosen randomly (by hand) and the net helicity was zero. Very quickly the helicity picture changes. From a zero helicity spectrum, soon helicity of opposite sign appears in shells on opposite sides of the initial energy shell. For a short period, time sequences show that the helicity peak at higher wave number moves to small scales until it dissipates, leaving a net helicity of the sign of the large-scale peak. It is during this phase that the relative dissipation rate (dissipation/energy) is largest. Therefore, through dissipation of helicity at small scales, large-scale helicity is generated. Once only the large-scale helicity peak is left, the blocking action of the helicity at large scales becomes important and the dissipation rate is suppressed.

In case D, the helicity of each mode is chosen to be zero by using free-slip boundary conditions in along central planes in the box. All the modes except one use the same free-slip symmetry plane, with the exception imposed to break this symmetry. From these initial conditions helicity does not initially grow around the initial $k=4$ wave number band, but around the resonance band at $k=8$. Note that once again helicity first appears in neighboring bands with opposite signs. Then time sequences show that the bands move toward opposite ends of the spectrum. Once again, dissipation is largest when the high wave number helicity band moves into the dissipation band and is annihilated, then decreases when large-scale helicity of only one sign remains.

To make this more quantitative, more calculations need to be done, as well as an analysis of helicity spectra and transfer properties. But what of a relationship to the shell models? Investigations of shell models with many more than two variables per shell seem invariably to lead to reductions in intermittency. Fully developed turbulence when viewed as a shell model has an infinite number of degrees of freedom and should in this sense not be intermittent. But it is, and this is understood as being due to coherent structures in physical space, which in Fourier space implies strong phase correlations. The phase correlations therefore prune the number of paths the cascade can take, returning us to simple models with few paths and strong intermittency, such as those presented here. Therefore, to obtain meaningful comparisons between 3D direct calculations and shell models, there must be some means of identifying the paths the cascade will follow, and calculating statistics along these paths. Given the difficulty of attaining this, let us make some other suggestions.

First, there needs to be further work on bidimensional correlations of wave number and time, similar to Fig. 3 here, and in earlier analysis [12,13]. The question with direct calculations is what quantities to use. It has been found [12] that energy-transfer spectra have a strong signature. Helicity spectra and helicity transfer spectra need to be analyzed in the same manner. For simulations with a small number of initial modes, such as the examples just given, at least for short times statistics for modes formed by the initial interactions and their daughters could be studied. It is our hope that analysis of Navier-Stokes simulations of this type, coupled with any additional understanding of the role of helicity coming from shell models, will provide insight into the nature of the intermittent cascade of energy to small scales in turbulent flows.

ACKNOWLEDGMENTS

We thank Detlef Lohse, Leo Kadanoff, and Norbert Schoerghofer for having communicated to us their numerical data before publication. We also thank Roberto Benzi, Uriel Frisch Detlef Lohse, Leo Kadanoff, Giovanni Paladin, Norbert Schoerghofer, Elisabetta Trovatore, and Angelo Vulpiani for useful discussions. One of us (L.B.) has been partially supported by the EEC Contract No. ER-BCHBICT941034. NCAR is supported by the National Science Foundation.

[1] E. B. Gledzer, Dok. Akad. Nauk SSSR **209**, 1046 (1973) [Sov. Phys. Dokl. **18**, 216 (1973)].
[2] K. Ohkitani and M. Yamada, Prog. Theor. Phys. **81**, 329 (1989); M. Yamada and K. Ohkitani, J. Phys. Soc. Jpn. **56**, 4210 (1987); Phys. Rev. Lett. **60**, 983 (1988); Prog. Theor. Phys. **79**, 1265 (1988).
[3] F. Waleffe, Phys. Fluids A **4**, 350 (1992).
[4] J. C. André and M. Lesieur, J. Fluid Mech. **81**, 187 (1977).
[5] W. Polifke and L. Shtilman, Phys. Fluids A **1**, 2025 (1989).
[6] H. K. Moffatt, J. Fluid Mech. **35**, 117 (1969).
[7] L. Kadanoff, D. Lohse, J. Wang, and R. Benzi, Phys. Fluids **7**, 617 (1995).
[8] R. M. Kerr and E. D. Siggia, J. Stat. Phys. **19**, 543 (1978).
[9] V. N. Desnyansky and E. A. Novikov, Prinkl. Mat. Mekh.

38, 507 (1974) [J. Appl. Math. Mech. **38**, 507 (1974)]; V. N. Desnyansky and E. A. Novikov, Atmos. Oceanic Phys. **10**, 127 (1974).
[10] F. H. Champagne, C. A. Friehe, J. C. LaRue, and J. C. Wyngaard, J. Atmos. Sci. **34**, 515 (1977).
[11] R. M. Kerr, J. Fluid Mech. **153**, 31 (1985).
[12] R. M. Kerr, J. Fluid Mech. **211**, 309 (1990).
[13] S. Kida and K. Ohkitani, Phys. Fluids **4**, 1602 (1992).
[14] F. Waleffe, Phys. Fluids A **5**, 677 (1993).
[15] J. Lee, J. Fluid Mech. **101**, 349 (1980).
[16] E. Leveque and Z.-S. She, Phys. Rev. Lett. (to be published).
[17] T. S. Lundgren, Phys. Fluids **25**, 2193 (1982).
[18] M. H. Jensen, G. Paladin, and A. Vulpiani, Phys. Rev. A **43**, 798 (1991).
[19] R. Benzi, L. Biferale, and G. Parisi, Physica D **65**, 163 (1993).
[20] D. Pisarenko, L. Biferale, D. Courvasier, U. Frisch, and M. Vergassola, Phys. Fluids A **65**, 2533 (1993).
[21] L. Biferale, A. Lambert, R. Lima, and G. Paladin, Physica D **80**, 105 (1995).
[22] O. Gat, I. Procaccia, and R. Zeitak (unpublished).
[23] E. Aurell, G. Boffetta, A. Crisanti, P. Frick, G. Paladin, and A. Vulpiani, Phys. Rev. E **50**, 4705 (1994).
[24] N. Schoerghofer, L. Kadanoff, and D. Lohse; Physica D **86**, 1 (1995).
[25] S. A. Orszag, in *Statistical Theory of Turbulence in Fluid Dynamics,* Proceedings of the Les Houches Summer School of Theoretical Physics, edited by R. Balian and J. L. Peube (Gordon and Breach, New York, 1977), p. 235.
[26] R. H. Kraichnan, J. Fluid Mech. **67**, 155 (1975).
[27] D. H. Porter, A. Pouquet, and P. R. Woodward, Theor. Comput. Fluid Dyn. **4**, 13 (1993).
[28] R. Benzi, L. Biferale, R. M. Kerr, and E. Trovatore (unpublished).
[29] H. Aref and I. Zadwadzki, Nature **354**, 50 (1991).
[30] M. V. Melander and F. Hussain (unpublished).
[31] U. Frisch, Z. S. She, and P. L. Sulem, Physica D **28**, 382 (1987).
[32] D. Lohse and A. Müller-Groeling, Phys. Rev. Lett. **74**, 1747 (1995).

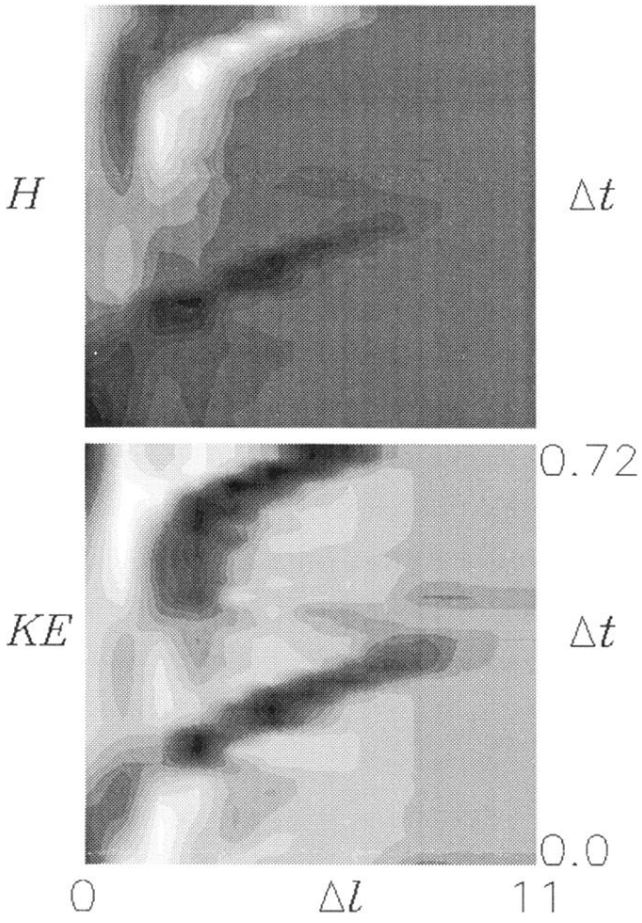

FIG. 3. Hovmüller diagrams in shell and time separation of kinetic energy and Hamiltonian fluctuations at different shell numbers and times using (4). Negative fluctuations correlation are light, positive are dark. Note the strong black for energy is not at (0,0), indicating that the strongest fluctuations in energy are in the higher shells. The sign of H fluctuations changes between pulses (light upper ridge), but does not for energy (dark upper ridge).